Supporting Information

Defect-enriched Active Self-supported Coralline-like High-Entropy Spinel Oxide $(FeNiCoMnCr)_3O_4$ electrodes for High-stability Oxygen Evolution Reaction

Lei He[a1], Huiyang Zhao[b1], Hongjun Kang[b,*], Hengjia Liu[a], Kai Cui[b], Jiaqi Chen[b], Wei Qin[a,*], and Xiaohong Wu[b,*]

[a]School of Materials Science and Engineering, Harbin Institute of Technology, Harbin, Heilongjiang 150001, P. R. China.

[b]School of Chemistry and Chemical Engineering, Harbin Institute of Technology, Harbin, Heilongjiang 150001, P. R. China.

1These authors contributed equally to this work and should be considered co-first authors

*Correspondence: kanghj@hit.edu.cn (H. Kang)

qinwei@hit.edu.cn (W. Qin)

wuxiaohong@hit.edu.cn (X. Wu)

Table S1 Specific surface areas of the catalysts.

Catalysts	HEO@NF	HEO-H400@NF	HEO-H500@NF	HEO-H600@NF
$S_{BET}(m^2/g)$	17.486	24.164	42.515	38.778

Table S2 XPS Analysis of Ni Elements on nickel foam self-supported electrode after H_2 treatment at different temperatures

Sample	Ni(852.5 eV)	Ni^{2+}（854.85 eV）	Ni^{3+}（856.60 eV）
HEO@NF	--	41.13	58.87
HEO-H400@NF	16.31	44.37	39.32
HEO-H500@NF	16.30	48.08	35.62
HEO-H600@NF	33.83	25.63	40.55

Table S3 XPS Analysis of HEO@NF and HEO-H500@NF

Element	HEO@NF	HEO-H500@NF
Fe^{2+}(710.5 eV)	69.43	49.69
Fe^{3+}(712.5 eV)	30.57	50.31
Ni (852.5 eV)		16.30
Ni^{2+}(854.85 eV)	41.13	48.08
Ni^{3+}(856.60 eV)	58.87	35.62
Co^{2+}(782.2 eV)	48.15	40.75
Co^{3+}(780.2 eV)	51.85	59.25
Mn^{3+}(641.7 eV)	60.74	76.54
Mn^{4+}(644.8 eV)	39.26	23.46
Cr^{3+}(576.2 eV)	64.12	55.81
Cr^{6+}(578.3 eV)	35.88	44.19

Table S4 TOF values for all samples

Sample	j at overpotential of 300 mV.(mA/cm^2)	TOF(s^{-1})
HEO@NF	11	3.31
HEO-400@NF	22	6.62
HEO-500@NF	270	81.33
HEO-600@NF	105	31.63
HEO-500+NF	44	13.25

Table S5 Overpotential and tafel slope of spinel metal oxides reported in this paper and literature at 100 mA cm^{-2} (All electrolytes were 1 M KOH)

Catalyst	Overpotential at 100 mA cm^{-2} (mV)	Tafel Slope (mV dec^{-1})	Reference
HEO-H500@NF	280	40.3	This work
$(FeNiCoCuV)_3O_4$	308	48.5	[1]
$(FeCoNiMnZn)_3O_4$	422	53	[2]
$(FeCoNiCrMn)_3O_4$	300	41.2	[3]
S-$(FeNiCoMnCr)_3O_4$	285	32.3	[4]
$(FeNiCoMnCr)_3O_4$	340	53.7	[5]
$(FeCoNiCrMn)_3O_4$	300	52.4	[6]
$(Co\,Mn_3NiFeZn)_3O_4$	410	53.5	[7]

Table S6 Overpotential and tafel slope of self-supporting high entropy electrode reported in this paper and literature at 100 mA cm^{-2}(All electrolytes were 1 M KOH)

Catalyst	Overpotential at 100 mA cm^{-2} (mV)	Tafel Slope (mV dec^{-1})	Reference
HEO-H500@NF	280	40.3	This work
$(CrMnFeCoCu)_3O_4$@CC	380	59.4	[8]
$(FeCoMnZnMg)_3O_4$@NF	390	59	[9]
FeCoNiCrMn HEA@NF	＞320	64.3	[10]
$AlFeCoNi_3Mo_{0.2}$ HEA	370	72	[11]
AlCoCrFeNi HEA	366	53.4	[12]
NiCoFeMnCrO@NF	294	46.7	[13]
CoCrFeNiNb HEA	304	42.7	[14]
FeCoNiCrMn HEA@NF	355	49.29	[15]

Table S7 Equivalent Circuit Parameters for Samples of HEO-HX@NF

Sample	Rs(Ω)	Rct (Ω)	Cdl-T	Cdl-P
HEO@NF	1.329	224.9	0.093277	0.74671
HEO-H400@NF	1.378	22.39	0.17609	0.82518
HEO-H500@NF	1.315	11.26	0.10813	0.82345
HEO-H600@NF	1.157	12.59	0.0931	0.83714

Table S8 XPS Analysis of HEO-H500@NF before and after OER

Element	Before OER（at.%）	After OER（at.%）
Fe^{2+}(710.5 eV)	45.19	49.69
Fe^{3+}(712.5 eV)	54.81	50.31
Ni(852.5 eV)	16.30	--
Ni^{2+}(854.85 eV)	48.08	38.18
Ni^{3+}(856.60 eV)	35.62	68.12
Co^{2+}(782.2 eV)	40.75	16.35
Co^{3+}(780.2 eV)	59.25	83.65
Mn^{3+}(641.7 eV)	76.54	66.43
Mn^{4+}(644.8 eV)	23.46	33.57
Cr^{3+}(576.2 eV)	55.81	35.30
Cr^{6+}(578.3 eV)	44.19	64.70

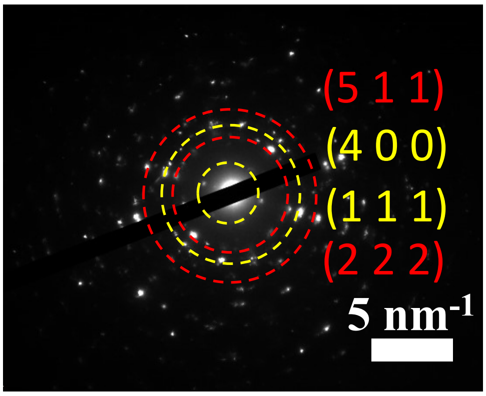

Fig. S1 SEAD image of HEO-H500@NF electrode.

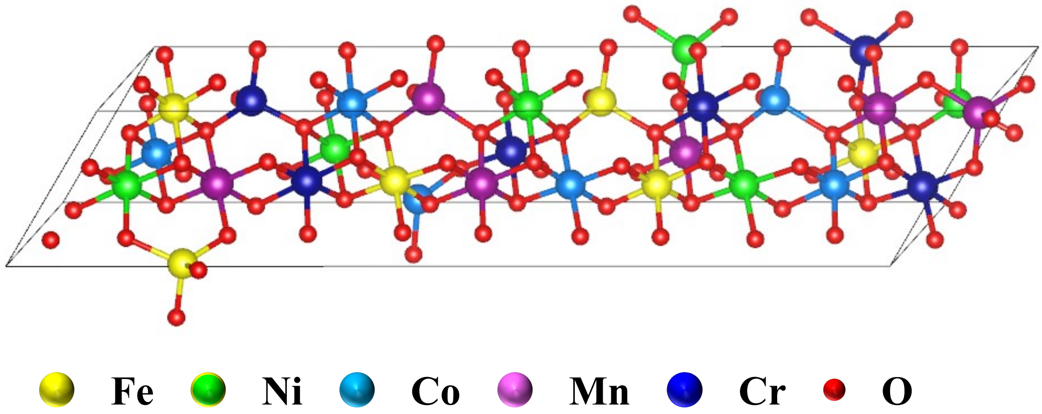

Fig. S2 XRD calculation model of $(FeNiCoMnCr)_3O_4$

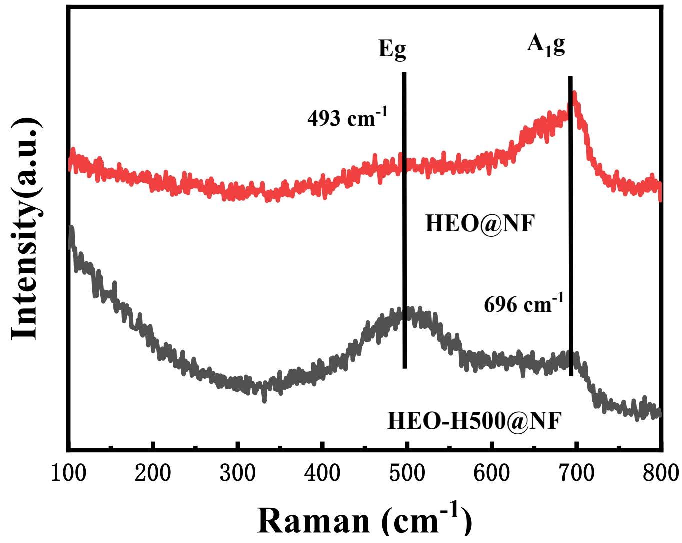

Fig. S3 Raman of HEO@NF and HEO-H500@NF

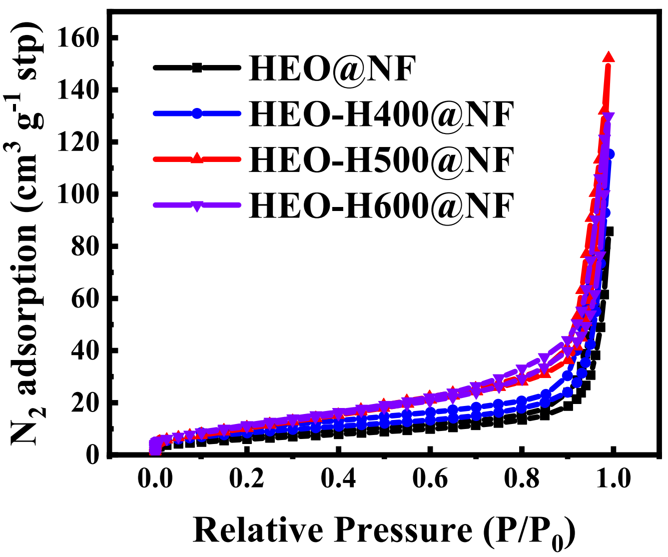

Fig. S4 Nitrogen adsorption-desorption isotherms of self-supported foam nickel electrode after H2 treatment at different temperatures

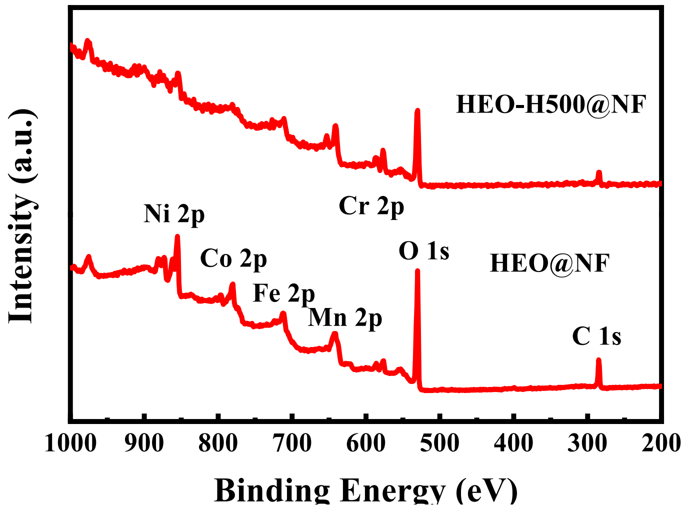

Fig. S5 XPS full spectra of HEO@NF and HEO-H500@NF

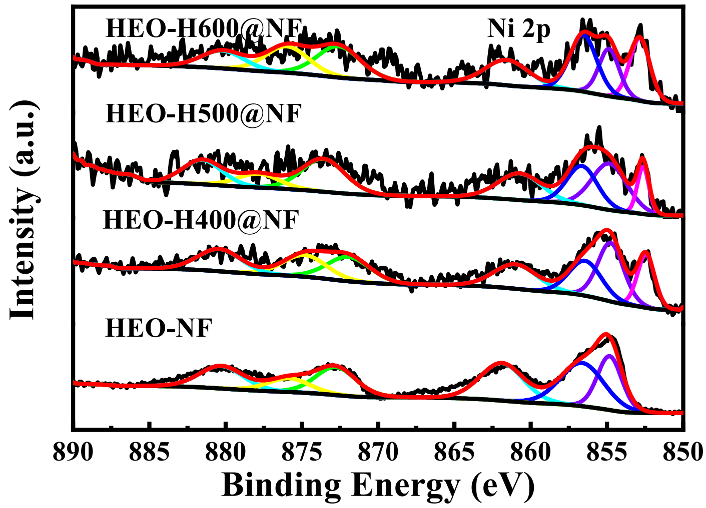

Fig. S6 High resolution Ni 2p spectra of nickel foam self-supported electrode after H_2 treatment at different temperatures

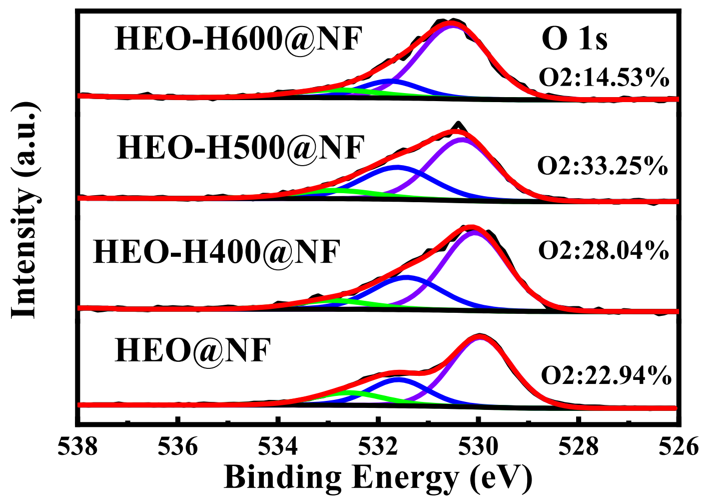

Fig. S7 High resolution O 1s spectra of nickel foam self-supported electrode after H_2 treatment at different temperatures

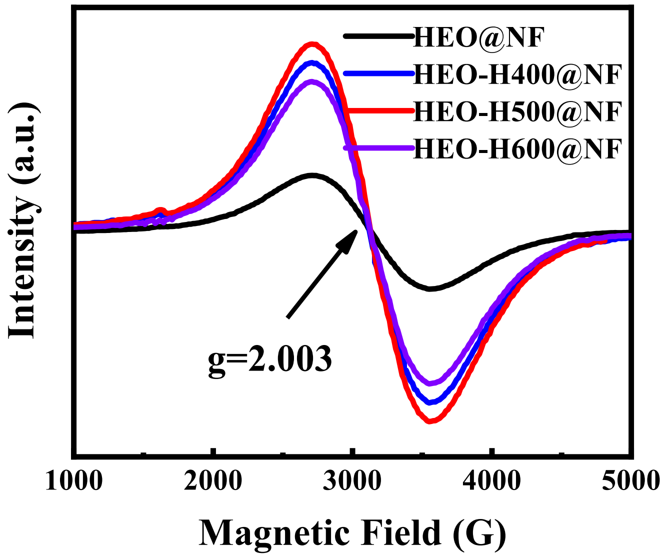

Fig. S8 ESR spectra of nickel foam self-supported electrode after H_2 treatment at different temperatures

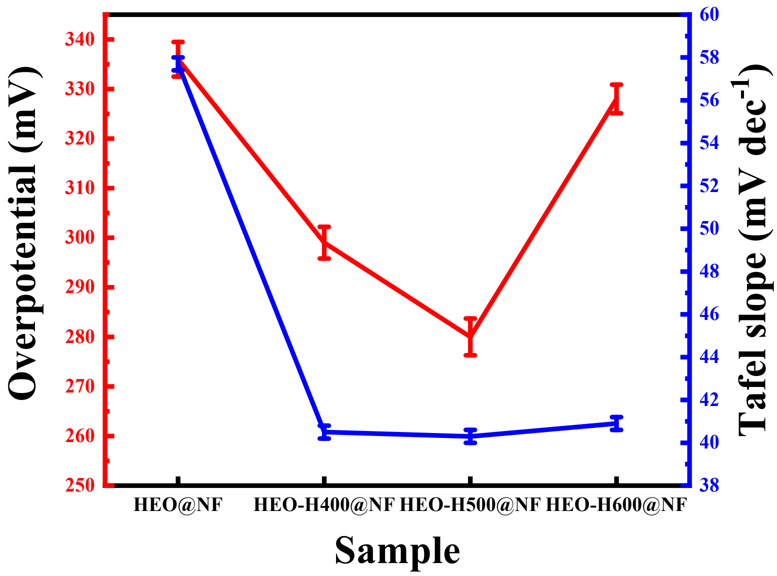

Fig. S9 Over potential(100 mA/cm^2) and Tafel slopes of the as-synthesized electrodes in 1.0 m KOH.

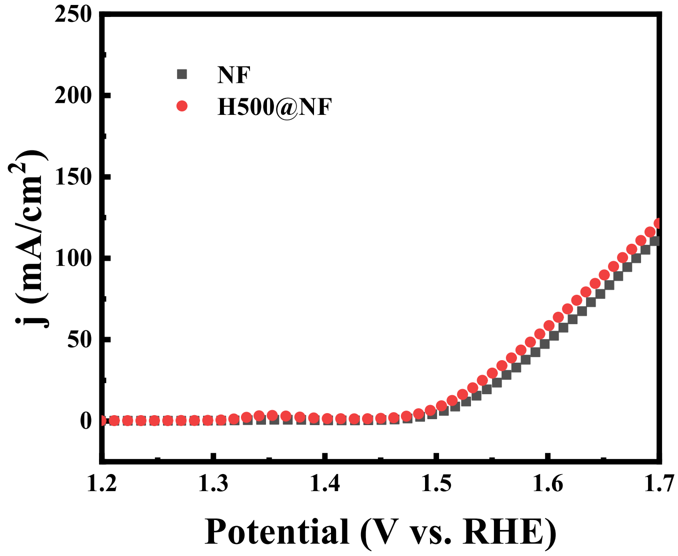

Fig. S10 Electrochemical performances of NF and H500@NF

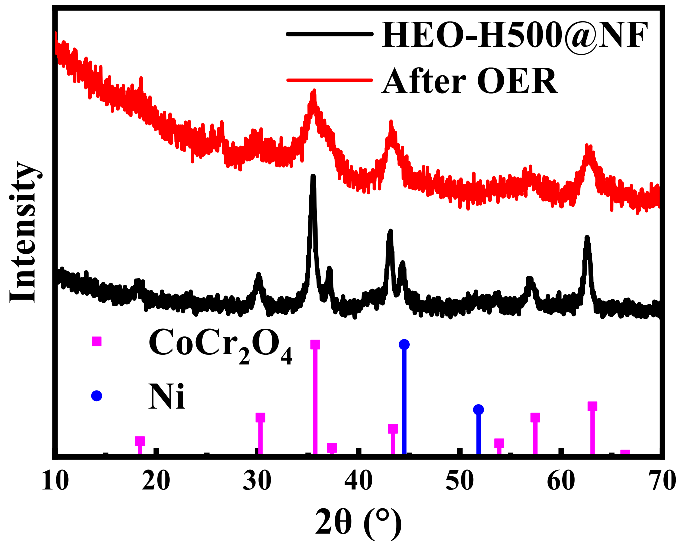

Fig. S11 XRD of HEO-H500@NF before and after activation

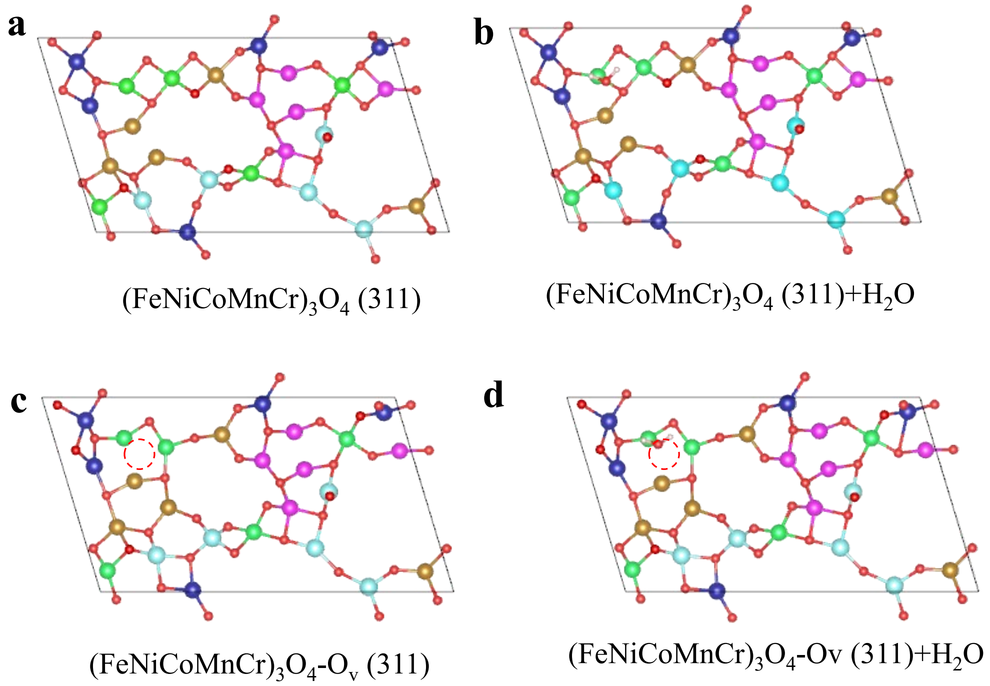

Fig. S12 The adsorption model of H_2O onto the (3 1 1) of (a, b) pristine $(FeNiCoMnCr)_3O_4$ and (c d) $(FeNiCoMnCr)_3O_4$-O_V. (C-axis projection)

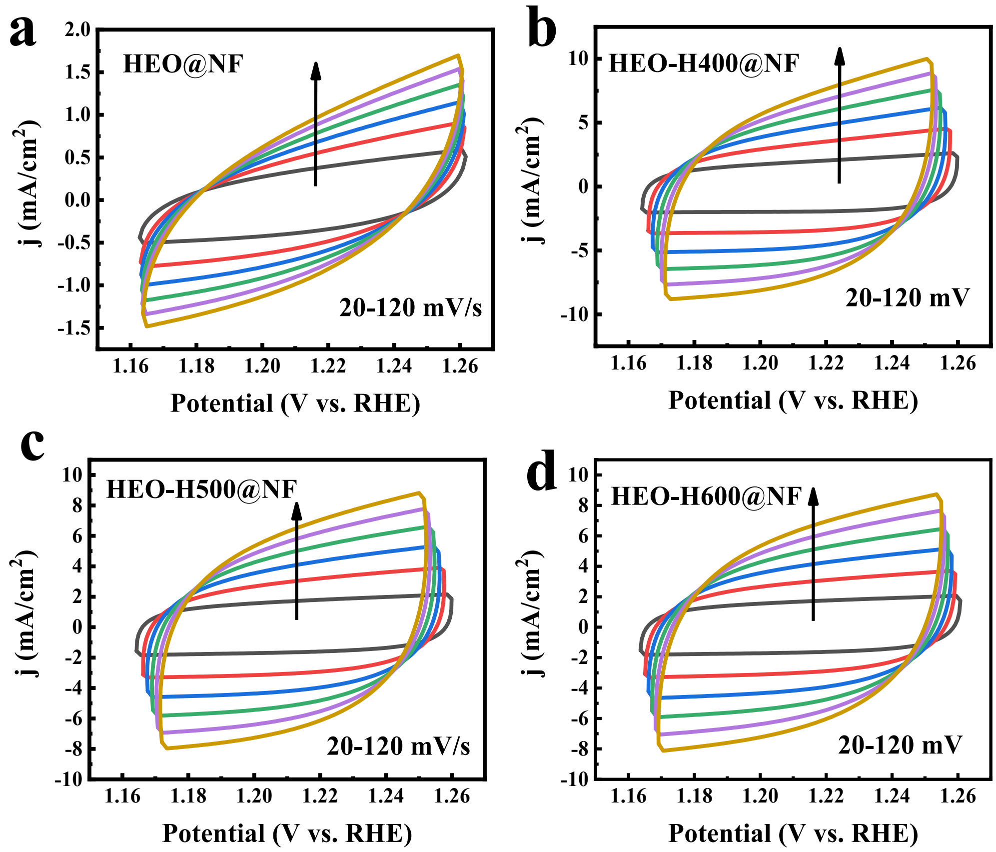

Fig. S13 The CV Cure of nickel foam self-supported electrode after H_2 treatment at different temperatures

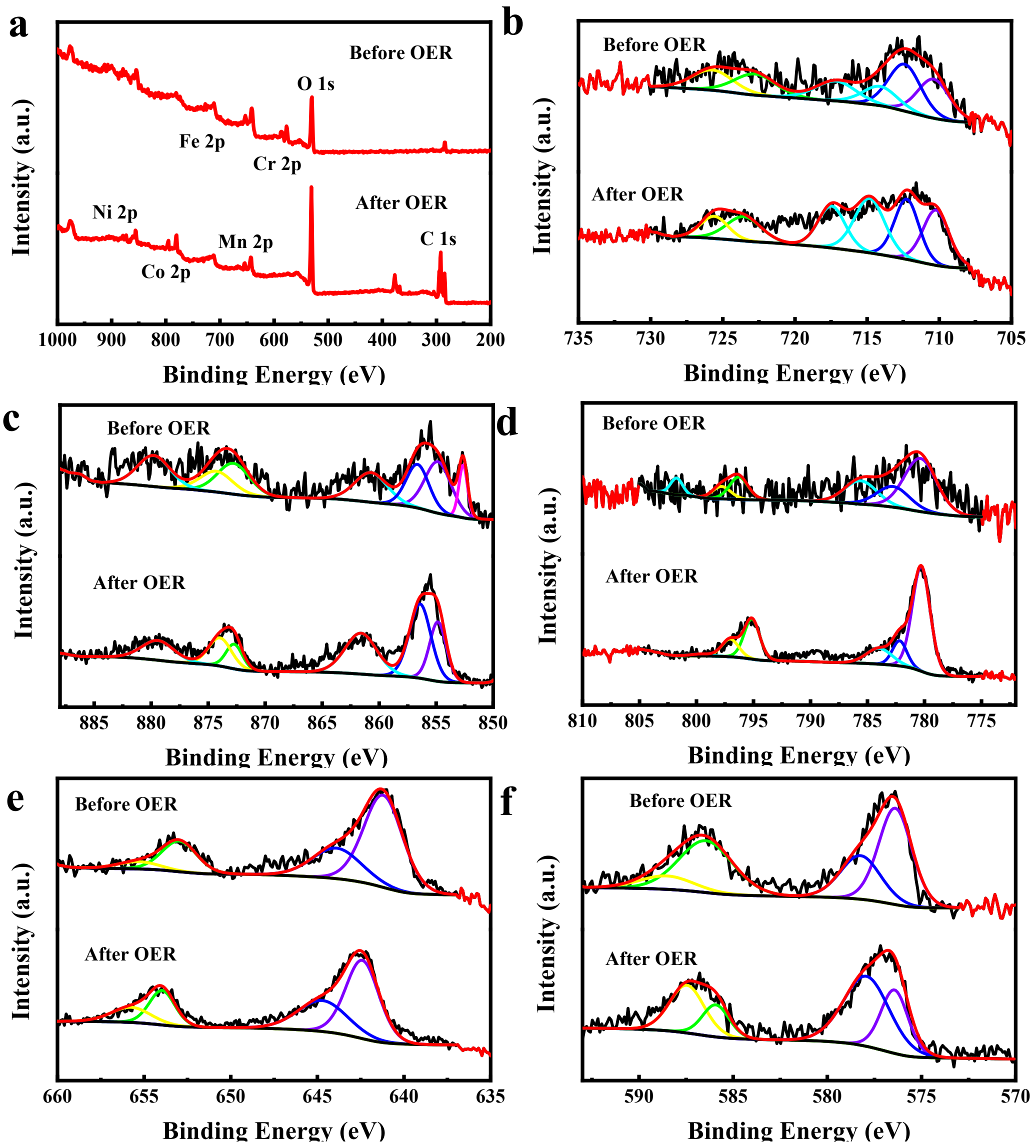

Fig. S14 XPS of HEO-H500@NF Before and after OER (a) full spectra (b) Fe 2p spectra (c)Ni 2p (d) Co 2p spectra (e) Mn 2p spectra (f) Cr 2p spectra

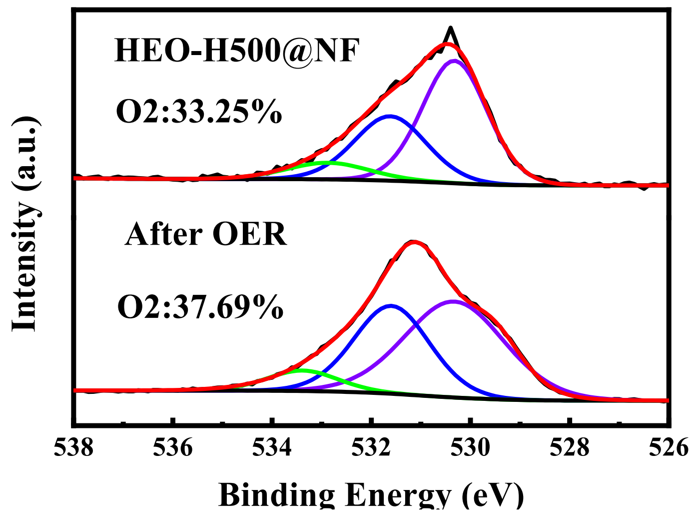

Fig. S15 Before and after OER O1s XPS of HEO-H500@NF

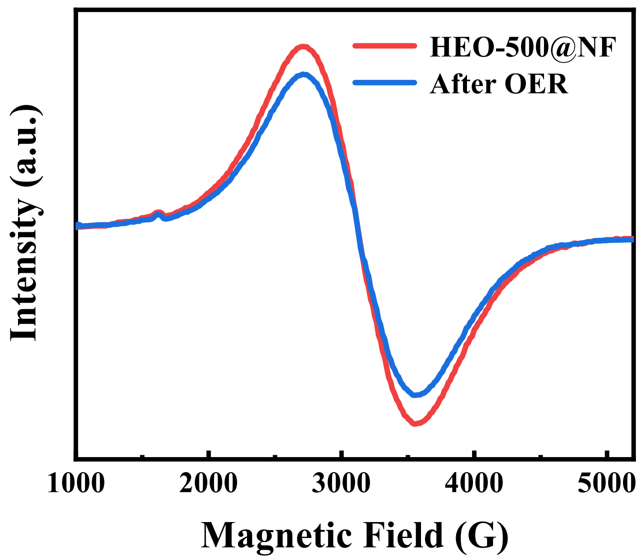

Fig. S16 ESR spectra of HEO-H500@NF before and after OER

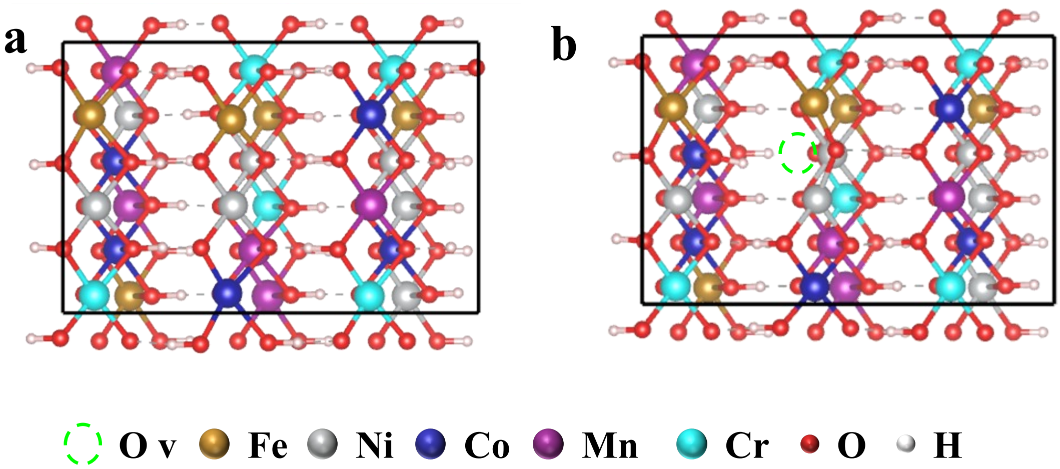

Fig. S17 The calculation model (a) (FeNiCoMnCr)(OH)x (b) (FeNiCoMnCr)(OH)x-Ov

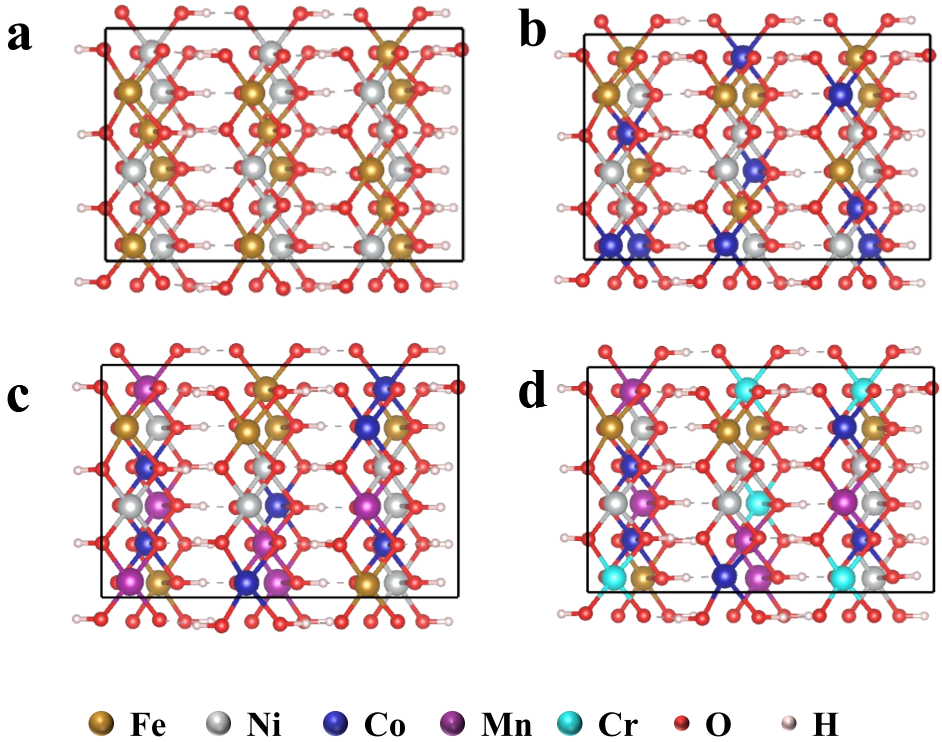

Fig. S18 The calculation model (a)(NiFe)(OH)x (b)(NiFeCo)(OH)x (c) (NiFeCoMn)(OH)x (d)(FeNiCoMnCr) (OH)x

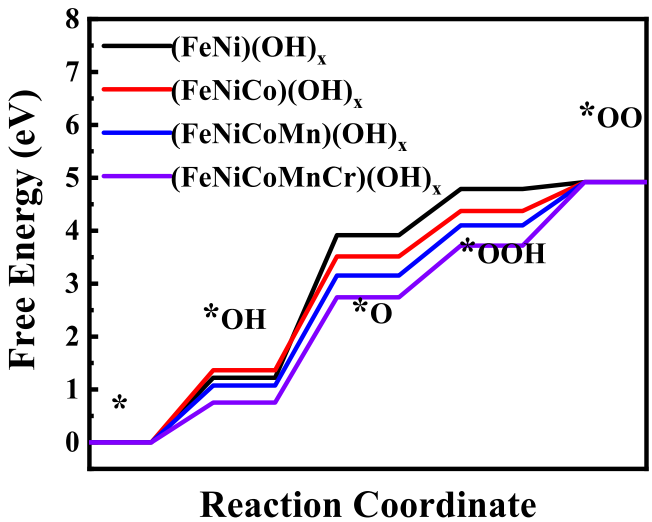

Fig. S19. Gibbs free energies diagram for the OER process catalyzed by (FeNi)(OH)x, (FeNiCo)(OH)x, (FeNiCoMn)(OH)x and (FeNiCoMnCr)(OH)x.

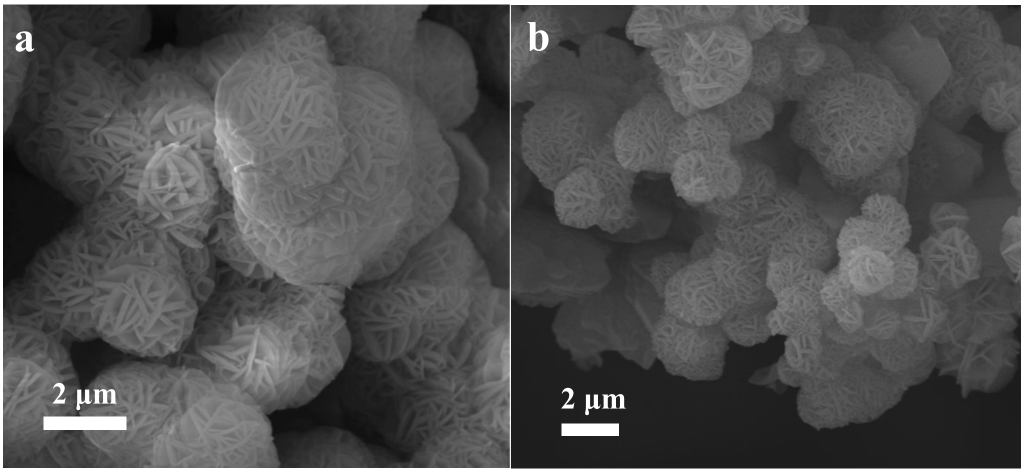

Fig. S20 SEM of HEO-H500@NF before and after activation (a)before OER (b)after OER

References

[1]Xuexue Wang, Lu Runqing, Gong Shanhe, et al. Identification of the reconstruction induced high-entropy spinel oxide nanosheets for boosting alkaline water oxygen evolution [J]. Chemical Engineering Journal, 2025, 503. https://doi.org/ 10.1016/j.cej.2024.158488

[2]Yifan Liu, Ye Caichao, Chen Long, et al. High Entropy‐Driven Role of Oxygen Vacancies for Water Oxidation [J]. Advanced Functional Materials, 2024, 34(25). https://doi.org/10.1002/adfm.202314820

[3]Huan He, Kou Pengzu, Zhang Zhigui, et al. Coupling high entropy oxide with hollow carbon spheres by rapid microwave solvothermal strategy for boosting oxygen evolution reaction [J]. Journal of Colloid and Interface Science, 2024, 653: 179-88. https://doi.org/ 10.1016/j.jcis.2023.09.063

[4]Dan Wang, Duan Chanqin, Yu Yihang, et al. Co-regulation of anion-cation in transition metal high entropy oxide for outstanding OER electrocatalytic performance [J]. Journal of Alloys and Compounds, 2023, 967. https://doi.org/ 10.1016/ j.jallcom.2023.171758

[5]Lei He, Kang Hongjun, Hou Guangyao, et al. Low-temperature synthesis of nano-porous high entropy spinel oxides with high grain boundary density for oxygen evolution reaction [J]. Chemical Engineering Journal, 2023, 460. https://doi.org/10.1016/j.cej.2023.141675

[6]Bomin Feng, Chen Jun, Yang Yifei, et al. Facile synthesis of nanosized spinel high entropy oxide $(FeCoNiCrMn)_3O_4$ for efficient oxygen evolution reaction [J]. Journal of Materiomics, 2024, 10(4): 919-27. https://doi.org/10.1016/j.jmat.2024.02.003

[7]Dongyuan Song, Liu Xueda, Wu Yingkai, et al. Optimizing d–p orbital hybridization by tuning high-entropy spinel oxides for enhanced alkaline OER efficiency [J]. Journal of Materials Chemistry A, 2025, 13(18): 13295-304. https://doi.org/10.1039/d4ta08485c

[8]Xuanmeng He, Zhang Zeqin, Jiang Xianwei, et al. Carbon cloth supporting $(CrMnFeCoCu)_3O_4$ high entropy oxide as electrocatalyst for efficient oxygen evolution reactions [J]. Journal of Alloys and Compounds, 2024, 1004. https://doi.org/10.1016/j.jallcom.2024.175874

[9]S. C. Karthikeyan, Ramakrishnan S., Prabhakaran S., et al. Low-Cost Self-Reconstructed High Entropy Oxide as an Ultra-Durable OER Electrocatalyst for Anion Exchange Membrane Water Electrolyzer [J]. Small, 2024, 20(45). https://doi.org/10.1002/ 10.1002/smll.202402241

[10]Peishu Yang, Shi Yongzhi, Xia Tongjun, et al. Novel self-supporting thin film electrodes of FeCoNiCrMn high entropy alloy for excellent oxygen evolution reaction [J]. Journal of Alloys and Compounds, 2023, 938. 168582

https://doi.org/10.1016/j.jallcom.2022.168582

[11]Qianqian Wang, Li Yongjie, Yang Yiyuan, et al. Self-supported AlFeNiCoMo high-entropy alloy with micropillar array structure for efficient oxygen evolution reaction [J]. APL Materials, 2022, 10(10). https://doi.org/10.1063/5.0117046

[12]Y. X. Yu, Xu J. L., Zhang L. W., et al. Electrochemically treated AlCoCrFeNi high entropy alloy as a self-supporting electrode for overall water splitting [J]. International Journal of Hydrogen Energy, 2024, 72: 209-19. https://doi.org/10.1016/j.ijhydene.2024.05.350

[13]Xin Li, Guo Si-Jia, Wu Zheng-Yi, et al. Multi-electron path modulation-activated LOM in self-supported high-entropy oxides for efficient oxygen evolution [J]. International Journal of Hydrogen Energy, 2025, 163. https://doi.org/10.1016/j.ijhydene.2025.150758

[14]Yuhan Lin, Xu Wence, Gao Zhonghui, et al. Self-supporting high-entropy Co-Cr-Fe-Ni-Nb oxide electrocatalyst with nanoporous structure for oxygen evolution reaction [J]. Chemical Engineering Journal, 2024, 489. https://doi.org/10.1016/j.cej.2024.151233

[15]Xiaorong Ruan, Wang Xiaohu, Zhang Guanhua, et al. Structure Engineering in Ion‐Beam Sputtered High‐Entropy Metallic Glass Electrocatalyst for Enhanced Oxygen Evolution [J]. Advanced Functional Materials, 2025. https://doi.org/10.1002/adfm.202511562